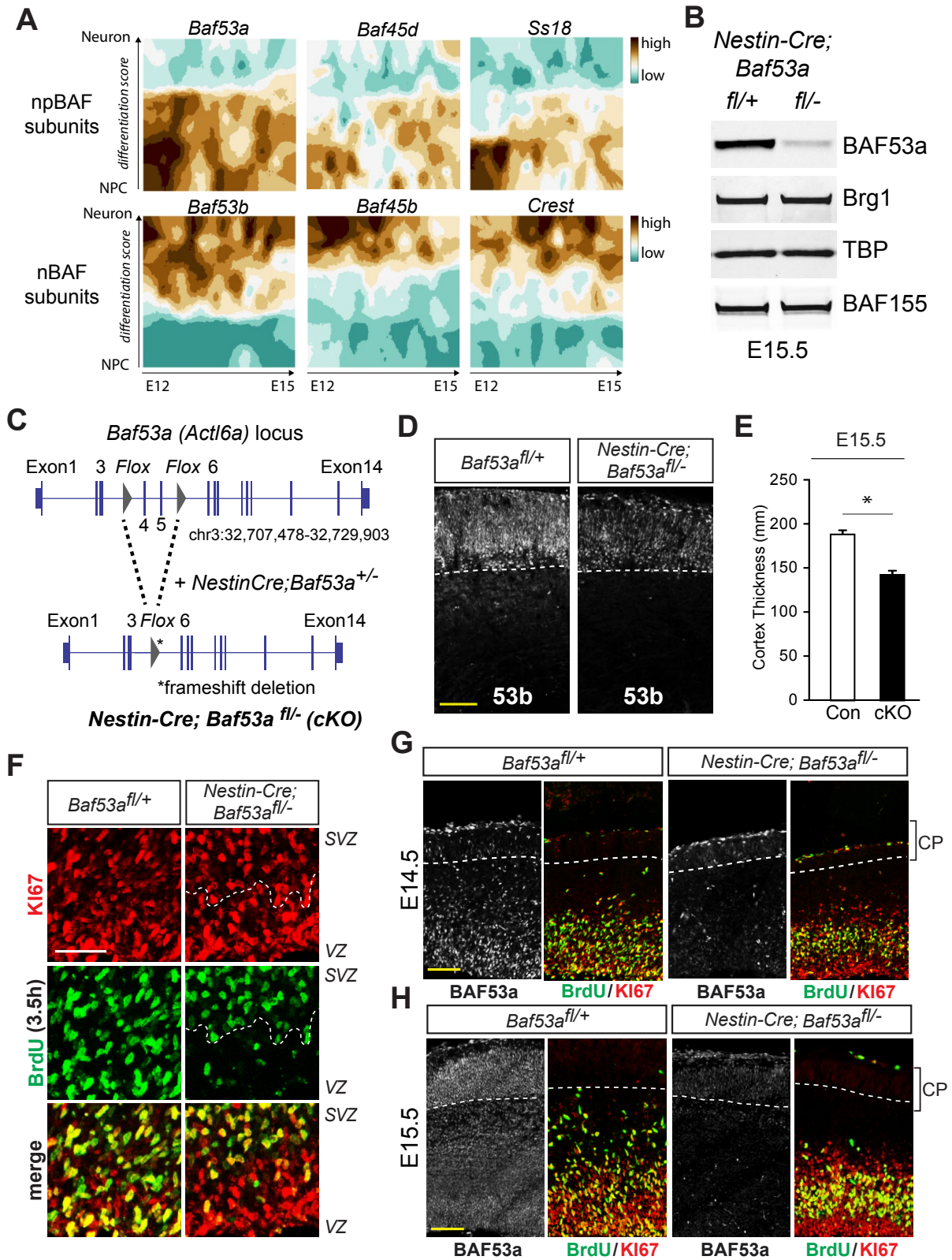


Supplemental Figures S1-S7



Supplemental Figure S1. BAF53a is required for normal neural development.

(A) Single cell RNA-seq data from Telley et al. Science (2019). Expression pattern of npBAF and nBAF subunits during embryonic neurogenesis from E12-E15.

(B) Western blot analysis from E15.5 mice forebrains showing significantly reduced levels of BAF53a in mutant cKO forebrains compared to controls. The levels of other BAF complex subunits, Brg1 and BAF155, are not changed.

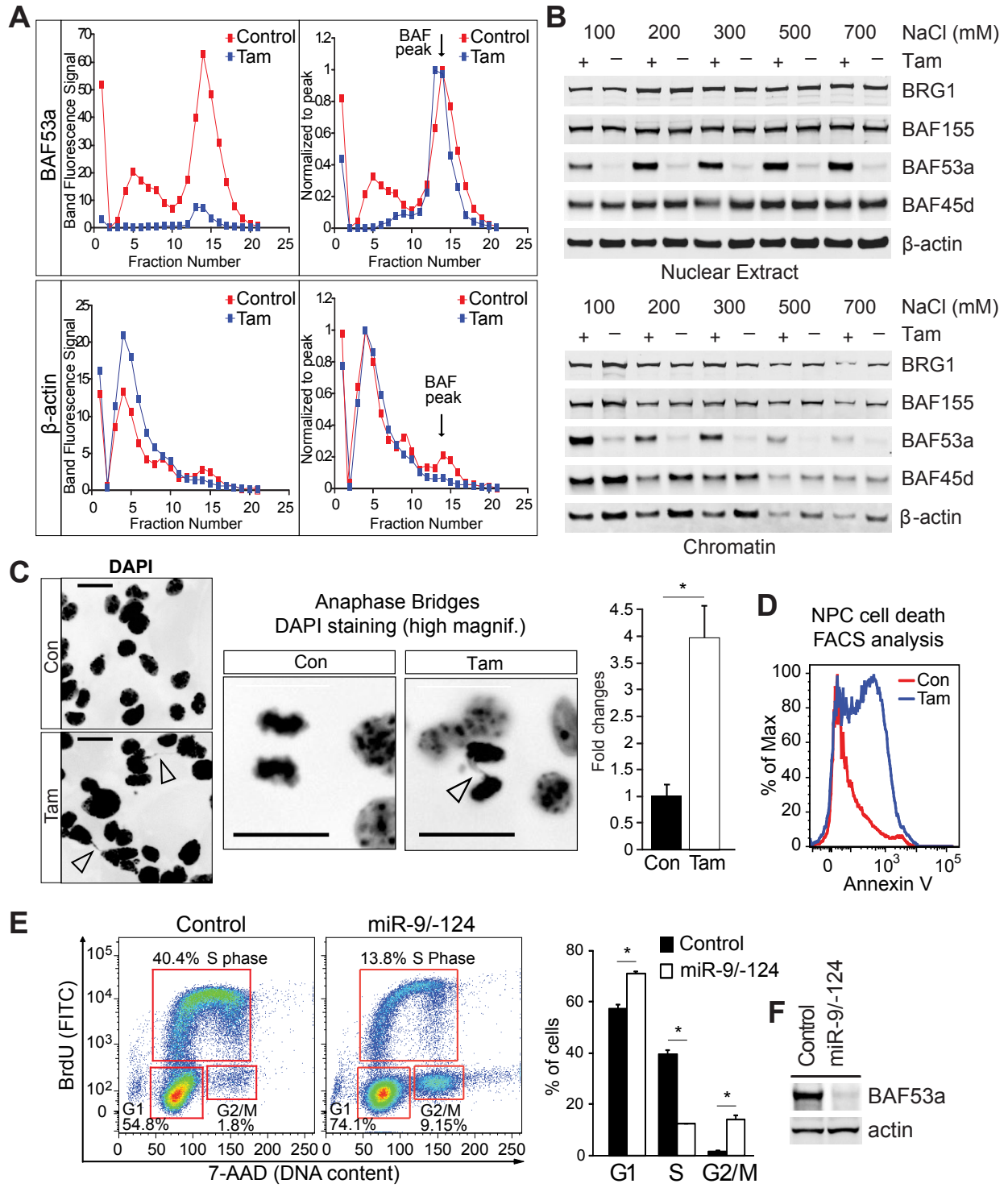
(C) Schematic representation of the BAF53a (*Actl6a*) locus after incorporation of *loxP* (*flox*) sequences flanking exons 4 and 5 (Krasteva et al. 2012). By breeding *Baf53a^{fl/-}* mice with *Nestin-Cre* expressing mice we generated brain specific BAF53a mutant mice.

(D) Immunofluorescence staining of coronal sections through E15.5 mouse cortex showing robust BAF53b expression in the cortical plate of control and BAF53a mutant brains. *Scale bar, 100μm.*

(E) Quantification of cortical thickness in E15.5 control and BAF53a mutant cortices. n=3, error bars represent SEM, *p<0.05.

(F) Immunostaining of E14.5 cortex for the proliferative marker KI67 (*red*) and short-term BrdU labeling (*green*, 3.5h pulse) highlighting a lack of marker co-localization in the ventricular zone of BAF53a mutants. *Scale bar, 50μm.*

(G,H) Immunohistochemistry of E14.5 (G) and E15.5 (H) mouse cortex showing reduced BAF53a expression in the ventricular zone of *Nestin-Cre;Baf53a^{fl/-}* brains compared to controls (*left panel*). Immunostaining for the proliferative marker KI67 (*red*) and short-term BrdU labeling (*green*, 3.5h pulse) (*right panel*). *Scale bar, 100μm.*



Supplemental Figure S2. Deletion of *Baf53a* does not affect BAF complex formation but results in an increase in anaphase bridges.

(A) Quantification of BAF53a and β -actin signals from glycerol gradient immunoblots shown in **Figure 1D** from control and BAF53a mutant cells. Signals were quantified and normalized to the peak value. Protein signal peaks from fraction 13-15 correspond to the BAF complex (*down arrows*).

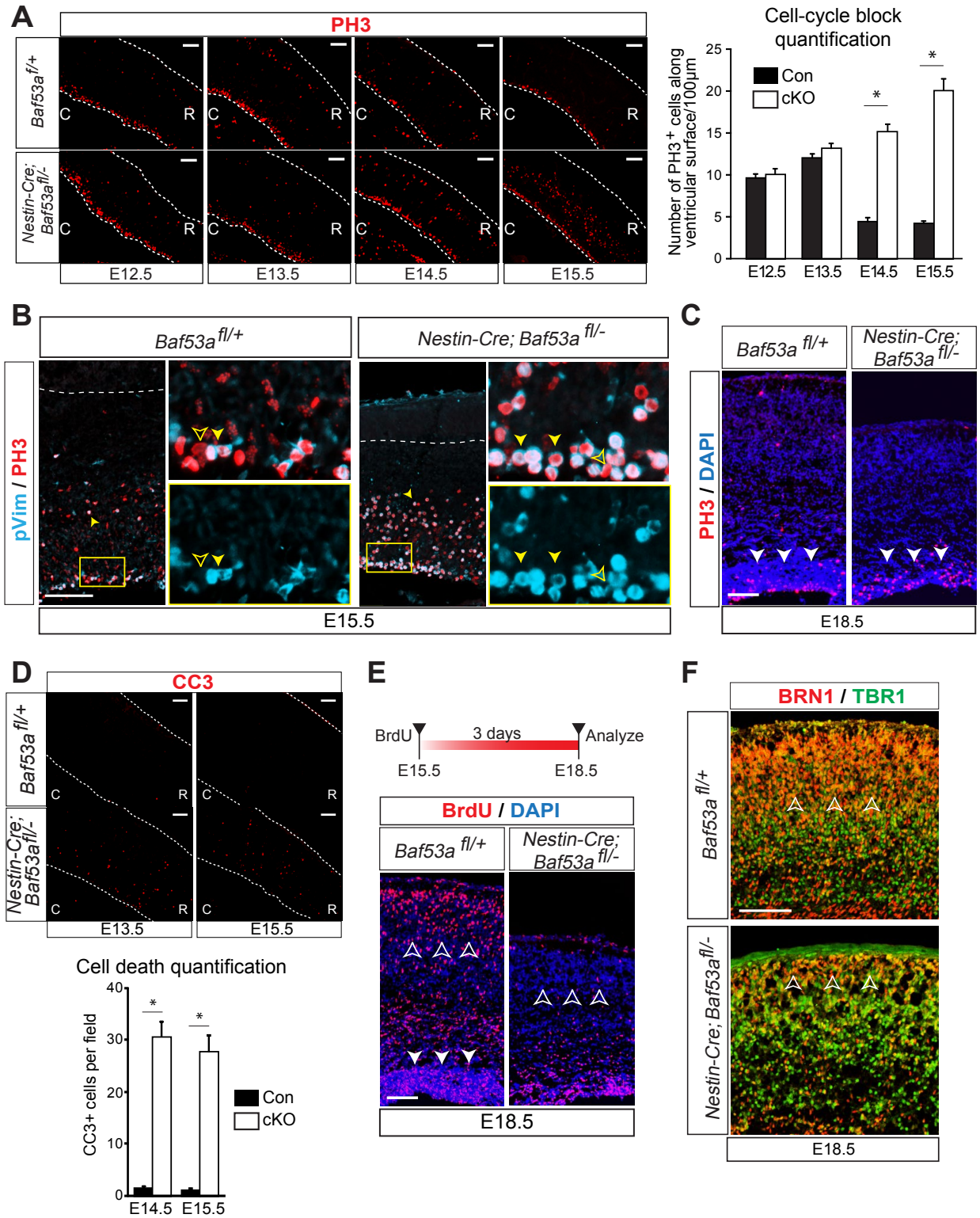
(B) Western blots examining the chromatin association of BAF complexes. Nuclei were prepared by hypotonic lysis and nuclear proteins were dissociated using varying concentrations of NaCl. Nuclear extract (supernatant) and chromatin (pellet) fractions were collected separately and analyzed by immunoblot using antibodies to different BAF complex components. +, control cells; -, BAF53a mutant cells.

(C) DAPI staining showing the decatenation defect following *Baf53a* deletion in neurospheres. Arrowheads indicate the DNA bridges (*left panel*) and M phase bridges (*right panel*), which are more often observed in the BAF53a mutant cultures. *Scale bar, 20 μ m*. Quantification of the relative number of DNA bridges between control and BAF53a mutant cells. n=3, error bars represent SEM, *p<0.05.

(D) FACS analysis for cell death using Annexin-V staining of NPCs following *Baf53a* deletion.

(E) Cell cycle FACS analysis of untransduced *Baf53a^{f/+}* neurospheres and *Baf53^{f/+}* neurospheres in which miR-9/-124 were prematurely expressed. Cells were incubated in BrdU 2 hours prior to collection and the fraction of cells in each stage of the cell cycle was assessed. Right panel: Quantification of the experiment. n=3, error bars represent SEM, *p<0.05.

(F) Western blot showing reduced levels of BAF53a in *Baf53a^{f/+}* neurospheres expressing miR-9/-124.



Supplemental Figure S3. Deletion of *Baf53a* leads to elevated pH3 staining and increased apoptosis.

(A) PH3 staining (*red*) of sagittal cortical sections from E12.5 to E15.5 BAF53a mutant and control mice. Dotted line contours the cortex spanning the ventricular wall to the pial surface. **R**, Rostral; **C**, Caudal. Scale bar, 50 μ m. Right panel: Quantification of PH3 (S10P, *red*) positive cells along the ventricular surface from E12.5 to E15.5. n=3, error bars represent SEM, *p<0.05.

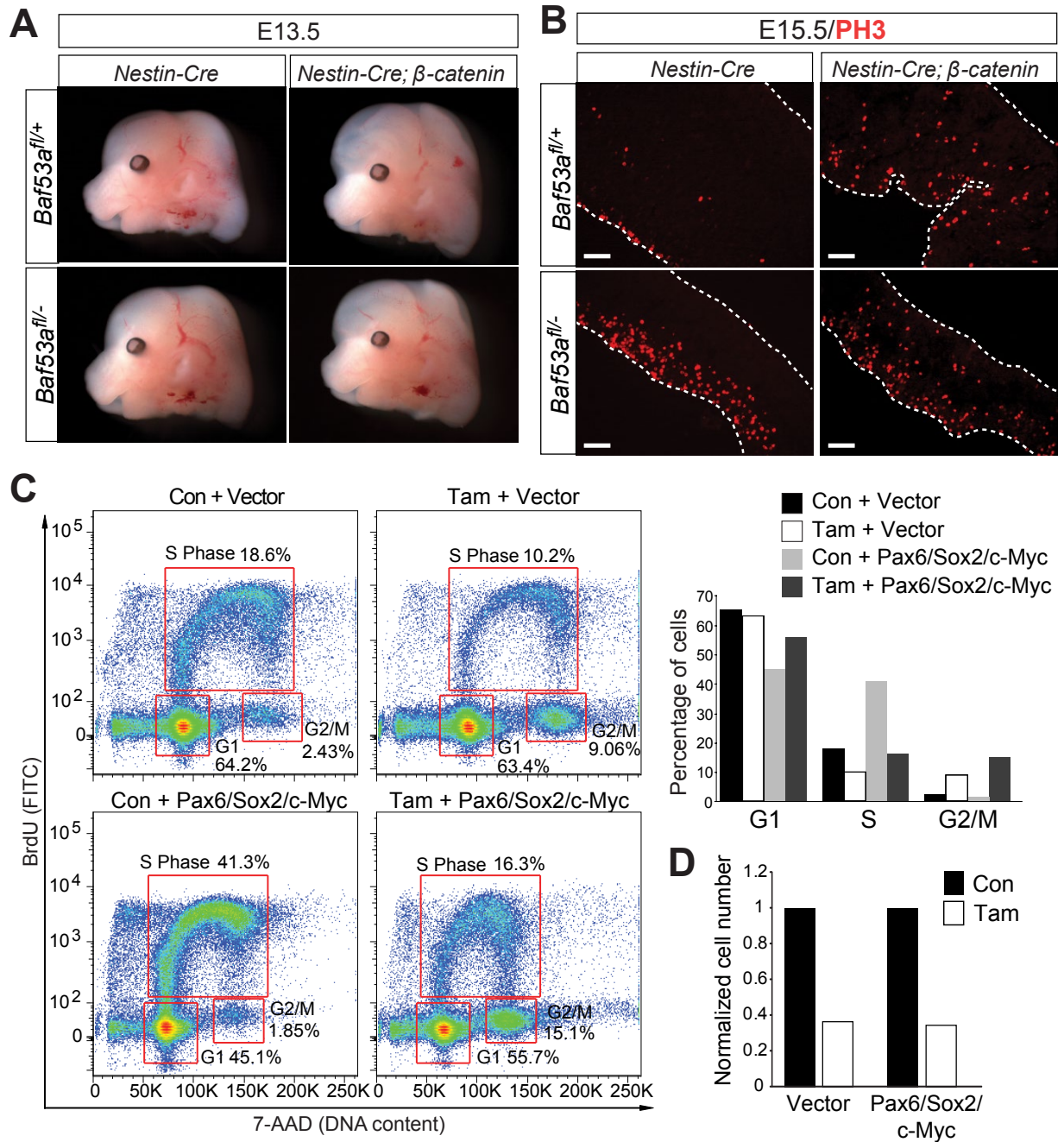
(B) Immunostaining for the radial glia marker phospho-Vimentin (pVim, *cyan*), which typically labels mitotic radial glia, and the mitotic indicator PH3 (*red*) highlights co-expression of both markers in E15.5 BAF53a mutant cortex, as well as the presence of many co-expressing cells in the SVZ (*inset and yellow solid arrow tip*). Scale bar, 100 μ m.

(C) Immunofluorescence staining of coronal sections through E18.5 mouse cortex showing persistent expression of the M-phase marker PH3 in BAF53a mutant brains. Scale bar, 100 μ m.

(D) Cleaved Caspase 3 (*red*) staining of E13.5 and 15.5 sagittal brain sections from *Nestin-Cre; Baf53a^{f/-}* and *Baf53a^{f/+}* embryos. Scale bar, 100 μ m. Right panel: quantification of CC3+ cell number in control and cKO brains. n=3, error bars represent SEM, *p<0.05.

(E) Immunostaining for BrdU+ (*red*) expressing cells in BAF53a mutant and control brains. The thymidine analog was administered at E15.5 and tissue harvesting was performed at E18.5 to determine the fate of the proliferating NPCs labelled at E15.5. Scale bar, 100 μ m.

(F) Immunostaining for BRN1 (*red*) and TBR1 (*green*) expressing cells in BAF53a mutant and control brains. BRN1-expressing cells are late-generated neuronal cell types which are dramatically reduced in BAF53a mutant brains. Scale bar, 100 μ m.



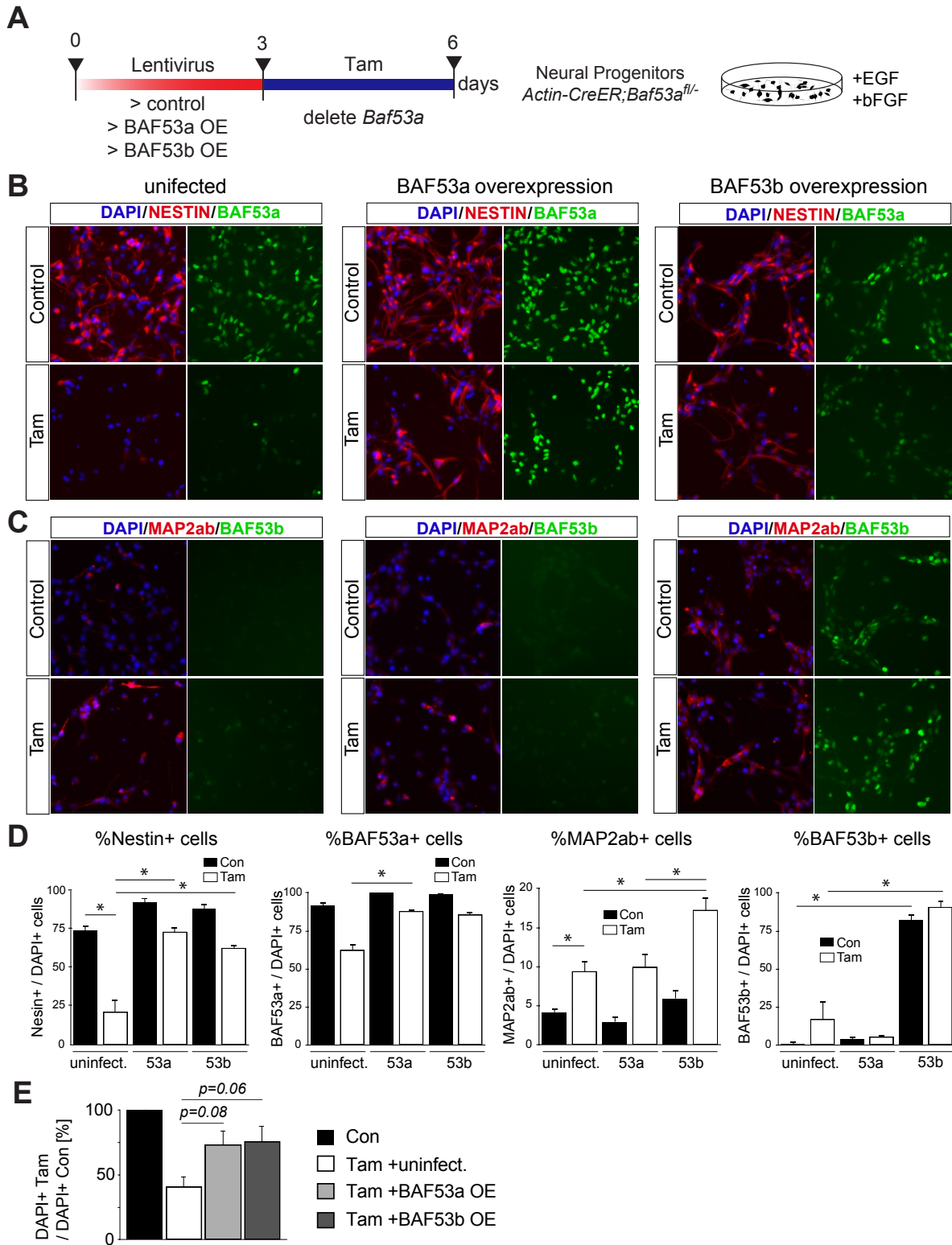
Supplemental Figure S4. Activation of β -catenin does not rescue deletion of BAF53a

(A) Microscopic images of E13.5 embryonic heads from *Baf53a* mutant and controls with or without the β -catenin transgene.

(B) Photomicrographs of sagittal sections from *Baf53a* mutant and control mice with or without the β -catenin transgene, stained for the M-phase marker PH3 (red). Scale bar, 100 μ m.

(C) Cell cycle FACS analysis of *Actin-CreER;Baf53a^{fl/-}* neurospheres treated with tamoxifen or vehicle and infected with empty vector or PMS factors (*Pax6*, *c-Myc* and *Sox2*). Cells were selected by a combination of blastomycin, hygromycin and puromycin prior to tamoxifen treatment. Infected cells were labeled with EdU for 2 hours for FACS analysis 72 hours after tamoxifen administration.

(D) Quantification of total cell numbers 72 hours after Tamoxifen treatment (normalized to condition treated with EtOH). n=2.



Supplemental Figure S5. BAF53b can rescue cell cycle block resulting from deletion of *Baf53a* by promoting neuronal differentiation of NPCs in vitro

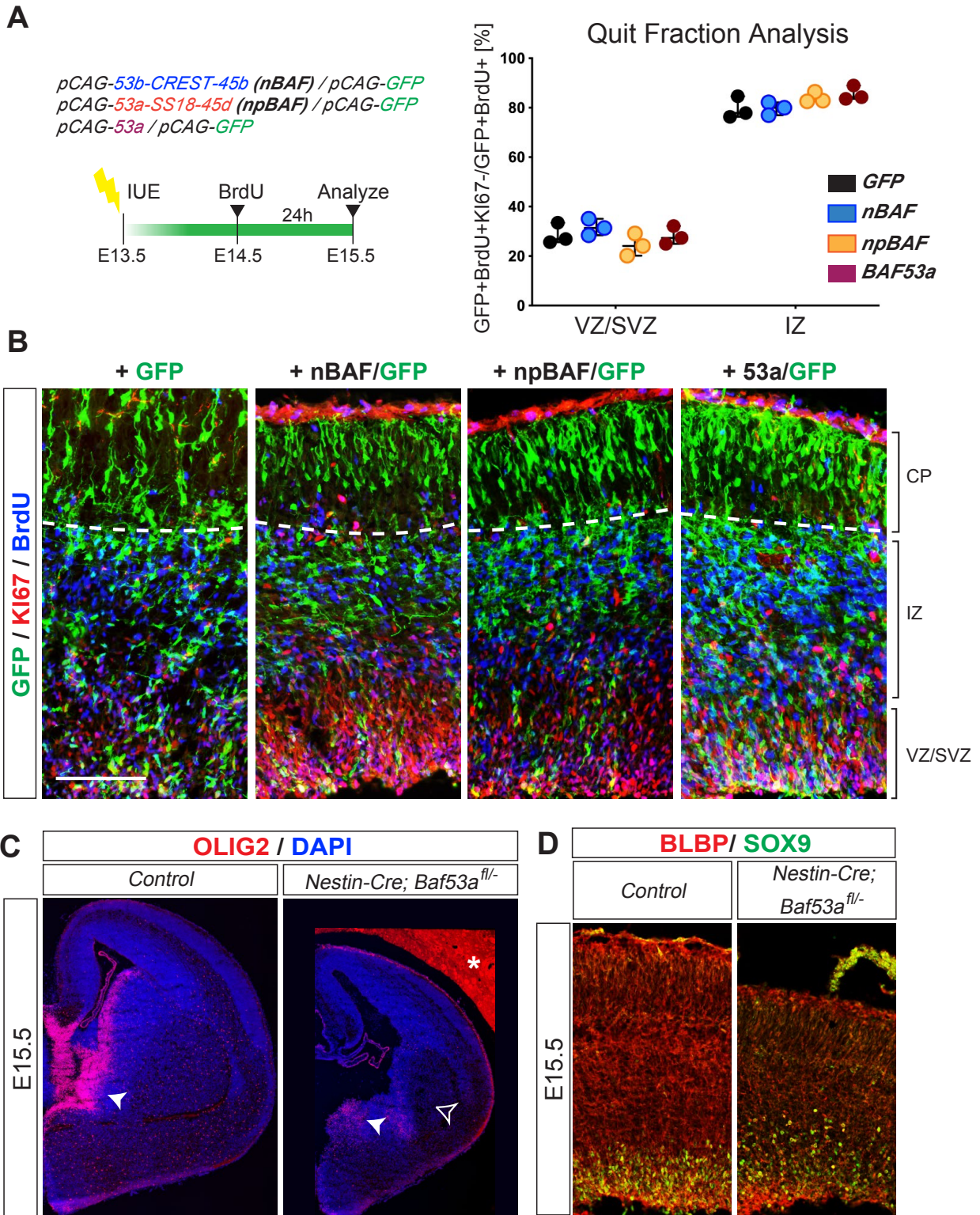
(A) Experimental setup for *in vitro* lentiviral rescue experiments overexpressing BAF53a or BAF53b following deletion of *Baf53a* in NPCs.

(B) Immunostainings for NESTIN (*red*) and BAF53a expressing cells (*green*) in control and tamoxifen treated conditions. Nestin is a marker for NPCs and its expression is markedly reduced following *Baf53a* deletion in NPCs. Overexpression of BAF53a or BAF53b significantly increases Nestin expression following *Baf53a* deletion.

(C) Immunostainings for MAP2AB (*red*) and BAF53b expressing cells (*green*) in control and tamoxifen treated conditions. MAP2ab is a marker for immature neurons and its expression is detected in 10% of cells following *Baf53a* deletion in NPCs. This induced neuronal differentiation is surprising as cells are maintained in proliferative EGF/bFGF containing media. Overexpression of BAF53b significantly increases MAP2ab expression following *Baf53a* deletion.

(D) Quantification of cells expressing NESTIN, MAP2AB, BAF53a and BAF53b. n=3, error bars represent SEM, *p<0.05, ANOVA and post-hoc Tukey's test for multiple comparisons.

(E) Quantification of the percentage of DAPI+ cells in Tamoxifen-treated or control cultures with and without BAF53a or BAF53b over-expression. n=3, error bars represent SEM, *p<0.05, ANOVA and post-hoc Tukey's test for multiple comparisons.



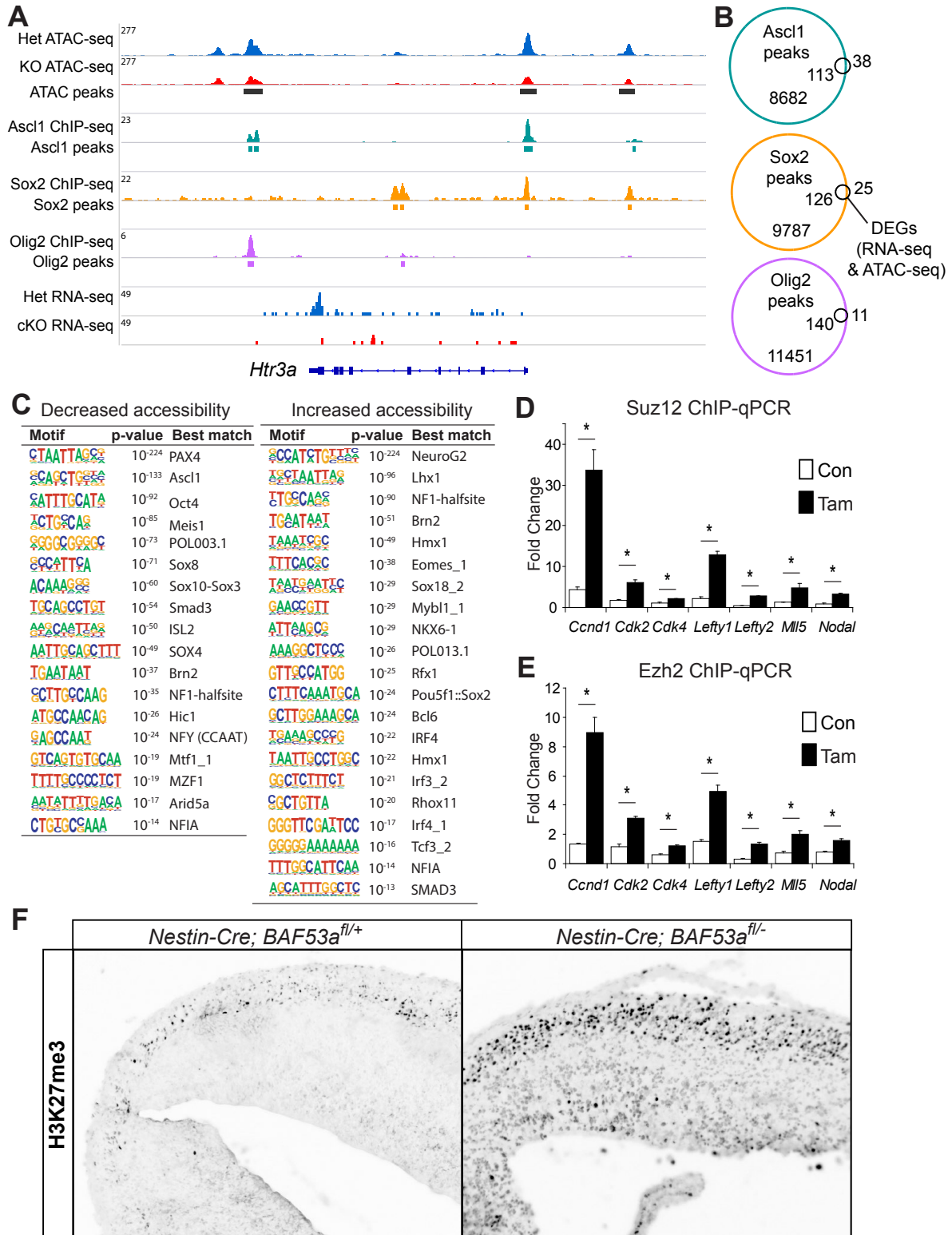
Supplemental Figure S6. Overexpression of nBAF or npBAF complex subunits, or BAF53a alone, in wild-type mice does not alter NPC cell cycle exit.

(A) Schematic of experimental paradigm and expression constructs used for *in utero* electroporation of Swiss Webster timed-pregnant dams at E13.5. Quantitative analysis of the fraction of electroporated cells to have exited the cell cycle within either the ventricular-subventricular (VZ/SVZ) or the intermediate germinal zones (IZ) indicate no change in cell cycle exit. Data presented as mean +/- SEM, no significant differences observed by one-way ANOVA and post-hoc Tukey's.

(B) Representative images of E15.5 coronal sections from the electroporated embryonic brains used for the cell fraction analysis in **(a)** immunostained for GFP (*green*), KI67 (*red*) and BrdU (*blue*). Scale bar, 100 μ m.

(C) Immunostaining for OLIG2 (*red*) expressing cells in BAF53a mutant and control brains at E15.5. Note asterisk (*) indicating non-specific background autofluorescent signal.

(D) Immunostaining for BLBP (*red*) and SOX9 (*green*) expressing cells in BAF53a mutant and control brains at E15.5.



Supplemental Figure S7. *Baf53a* deletion changes chromatin accessibility at proliferative and neurogenic gene loci by opposing Polycomb-dependent H3K27me3 repressive marks.

(A) Representative genome browser tracks showing ATAC-seq and RNA-seq peaks in cKO and Het forebrains, as well as Ascl1, Sox2 and Olig2 ChIPseq peaks from mouse NSPCs at the *Htr3a* locus.

(B) Venn diagrams comparing genes associated with Ascl1, Sox2 or Olig2 peaks to the list of 151 differentially regulated genes that showed changes in both RNA-seq and ATAC-seq in BAF53a cKO forebrains.

(C) Motif enrichment analysis of ATAC-seq datasets using HOMER software. Displayed are the TF motifs which are significantly enriched in peaks, which displayed either decreased or increased accessibility in BAF53a cKO brains.

(D,E) ChIP-qPCR analysis of SUZ12 (D) and EZH2 (E) levels at cell cycle regulator genes and stem/progenitor cell maintenance genes. The levels of these Polycomb Repressive Complex 2 (PRC2) subunits are increased at cell cycle genes following *Baf53a* deletion in *Actin-CreER;Baf53a^{f/f}* NSPCs. The PRC2 complex places repressive H3K27me3 marks on histones. n=3, error bars represent SEM, *p<0.05.

(F) Immunostaining for H3K27me3 expressing cells in BAF53a mutant and control brains at E15.5.